Biochemical and Biophysical Research Communications 456 (2015) 207–212

Contents lists available at ScienceDirect

Biochemical and Biophysical Research Communications

journal homepage: www.elsevier.com/locate/ybbrc

The pH-sensitive structure of the C-terminal domain of voltage-gated proton channel and the thermodynamic characteristics of Zn^{2+} binding to this domain

Qing Zhao, Chuanyong Li, Shu Jie Li *

Department of Biophysics, School of Physics Science, The Key Laboratory of Bioactive Materials, Ministry of Education, Nankai University, PR China

ARTICLE INFO

Article history:
Received 9 November 2014
Available online 24 November 2014

Keywords:
Voltage-gated proton channel Hv1
Carboxyl-terminal domain
pH
Zn^{2+}-binding
Isothermal titration calorimetry (ITC)

ABSTRACT

The voltage-gated proton channel Hv1 is strongly sensitive to Zn^{2+}. The H^+ conduction is decreased at a high concentration of Zn^{2+} and Hv1 channel closing is slowed by the internal application of Zn^{2+}. Although the recent studies demonstrated that Zn^{2+} interacts with the intracellular C-terminal domain, the binding sites and details of the interaction remain unknown. Here, we studied the pH-dependent structural stability of the intracellular C-terminal domain of human Hv1 and showed that Zn^{2+} binds to His^{244} and His^{266} residues. The thermodynamics signature of Zn^{2+} binding to the two sites was investigated by isothermal titration calorimetry. The binding of Zn^{2+} to His^{244} (mutant H266A) and His^{266} (mutant H244A) were an endothermic heat reaction and an exothermic heat reaction, respectively.

1. Introduction

Voltage-gated proton channel Hv1 is perfectively selective for protons and has no detectable permeability to other cations [1–5]. Hv1 is activated by depolarization and intracellular acidification [1,6], and the gating strongly depends on both the intracellular pH (pH_i) and extracellular pH (pH_o) [1,7]. Hv1 functions as a dimer and each subunit contains its own pore [8–10]. There is strong cooperativity between subunits in the dimeric Hv1. The activation of one monomeric channel subunit affects the gating of the other subunit within the dimeric architecture [11,12]. The intracellular C-terminal domain was found to be responsible for the dimeric architecture, cooperative gating, and structural stability of Hv1 [13,14].

Hv1 is strongly sensitive to polyvalent metal cations, particularly Zn^{2+} [1,2,4,5]. Extracellular Zn^{2+} blocks the channel at a low concentration and the inhibition is dependent on pH_o. The effect of external Zn^{2+} on the channel gating is profoundly enhanced at a high pH_o [15,16]. The pH-dependent inhibition suggests that Zn^{2+} blocks Hv1 by competing with H^+ for a site in the external surface of the channel, and two His residues, His^{140} and His^{193}, were found to be the sites contributing to the inhibition of extracellular Zn^{2+} [1,4,15,16]. In addition, it was previously shown that high concentrations of intracellular Zn^{2+} reduce Hv1 proton conduction and slow down channel closing [15]. In contrast with extracellular Zn^{2+}, intracellular Zn^{2+} has relatively weak and obviously different effects, indicating that extracellular and intracellular Zn^{2+} binds to different sites within Hv1 [15]. Although recent studies have shown that divalent metal ions interact with the C-terminal domain of Hv1 [17], the sites and thermodynamic signature of Zn^{2+} binding to the C-terminal domain remain unknown.

At some times, protein precipitation is induced by multivalent metal binding. In this process, multivalent metals serve as cross-linking agents between protein molecules, and the affinity of the protein for the metal, available metal coordination sites, protein and metal concentrations, and solution pH play important roles [18–20]. In the present work, we studied the pH-dependent structural stability of the intracellular C-terminal domain of human Hv1 and the binding of Zn^{2+} to the coiled-coil domain by Zn^{2+}-induced precipitation and isothermal titration calorimetry (ITC). We found that two His residues His^{244} and His^{266} are indispensable for Zn^{2+} binding. The binding of Zn^{2+} to His^{244} and His^{266} were an endothermic heat reaction and an exothermic heat reaction, respectively. Our results suggest that the two His residues within this domain may be the protonation sites that help regulate channel gating.

2. Materials and methods

2.1. Cloning, mutation, expression and purification

Gene cloning, expression and purification of the wild type C-terminal domain of Hv1 (residues 221–273) were the same as

* Corresponding author at: Department of Biophysics, School of Physics Science, Nankai University, 94 Weijin Road, Nankai District, Tianjin 300071, PR China. Fax: +86 22 2350 6973.
E-mail address: shujieli@nankai.edu.cn (S.J. Li).

http://dx.doi.org/10.1016/j.bbrc.2014.11.060
0006-291X/

described previously [21]. The point mutations in the protein (H244A, H266A and the H244A/H266A double mutant) were created by site-directed mutagenesis. Gene cloning, expression and purification of the mutants were the same as the wild type. Briefly, DNA fragments for the wild type and the mutants were inserted into a pGEX-6p-1 vector, respectively. Escherichia coli strain BL21(DE3) harboring the recombinant plasmids were grown in LB medium at 30 °C and induced with 0.5 mM IPTG at 25 °C for 20 h. The protein was purified with a Glutathione-Sepharose 4B affinity column (GE Healthcare), and GST-tag was removed by preScission protease. The C-terminal domain without the GST-tag was then purified by a High S Cartridge column (GE Healthcare), and a Superdex 75 10/300 gel filtration column (GE Healthcare). The concentrations of the proteins were determined by the BCA method using BSA as a standard.

2.2. Circular dichroism spectroscopy

CD measurements were carried out on an Applied Photophysics Chirascan CD spectrometer (Leatherhead, UK). CD data for far-UV (200–250 nm) were collected at 25 °C with a bandwidth of 0.5 nm using a quartz cuvette with a light path-length of 1 mm. The protein samples were diluted to 0.1 mg/ml with 50 mM sodium phosphate buffers containing 150 mM NaCl and 1 mM dithioerythritol (DTT) with a range of pH values of 5–8. The obtained values were subtracted by the corresponding baseline records for the buffers having the same concentration of salts under similar conditions.

2.3. Temperature-induced denaturation

The thermal melting experiments were carried out by increasing the temperature of the sample in the quartz cell with a path-length of 1 mm using a programmable water circulating bath. The temperature was increased from 25 to 90 °C at a rate of 1 °C/min. The measurements were performed with a step size of 5 °C and paused for 2 min at each temperature before recording. The sample was cooled to 25 °C for 5 min and taken a final measurement to determine the extent of refolding.

Denaturation curves were fitted to the two-state model [22]. The fraction unfolded, F_U, was calculated using Eq. (1):

$$F_U = [\theta_t - \theta_F]/[\theta_U - \theta_F] \quad (1)$$

where θ_t is the observed CD signals at any temperature; θ_F and θ_U are the signals for folded and unfolded state, respectively. The constant of folding for dimmer, K_F, is:

$$K_F = [F_2]/[U]^2 \quad (2)$$

where F_2 is the native dimer, U is the unfolded monomer. The thermal melting values, T_m (the midpoint of the thermal denaturation curve), can be derived using Eq. (3):

$$\Delta G = \Delta H(1 - T/T_m) - R \times T \times \ln P_t - \Delta C_p \times ((T_m - T) + T \times \ln(T/T_m)) \quad (3)$$

where ΔH is the enthalpy change; T is the absolute temperature; R is the ideal gas constant; ΔC_p is the change in heat capacity and P_t is the total protein concentration. The multi-wavelength temperature-dependent analysis was carried out using the Global 3™ global analysis software.

2.4. Zn^{2+} binding sites detected by SDS–PAGE

To determine qualitatively whether Zn^{2+} binds to His residues in the C-terminal domain of Hv1, the interactions of Zn^{2+} with the wild type, H244A, H266A and H244A/H266A, were estimated by SDS–PAGE. For pH 5, 10 mM sodium acetate buffer; for pH 6, 10 mM MES buffer; for pH 7–8, 10 mM HEPES buffer, containing 150 mM NaCl and 0.5 mM dithioerythritol (DTT), were used. The mixtures containing 0.5 mg/ml protein and various concentrations of $ZnCl_2$ were centrifuged at 12,000 rpm for 20 min. The proteins in supernatants and pellets were detected by SDS–PAGE.

2.5. Isothermal titration calorimetry

ITC measurements were carried out on a TAM III microcalorimetric system (TA instruments-Waters LLC, USA). The wild type C-terminal domain of Hv1 and the mutants (H244A, H266A, the H244A/H266A double mutant) were dissolved in buffer (20 mM HEPES buffer containing 100 mM NaCl and 0.5 mM DTT, pH 6.5), and dialyzed against the same solution. The titrant, chloride salt of Zn^{2+}, was dissolved in the buffer as mentioned above, and the concentration was adjusted to be 10–50-fold higher than the protein concentration. The protein samples and titrant were degassed at room temperature for 10 min before each titration. 800 μl of the protein samples at 50–100 μM was placed in the reaction cell. The titration was undertaken by injecting 8 μl × 25 injection of the titrant at 300-S intervals with stirring at 60 rpm to ensure a complete equilibration. Control experiments, that were used to determine the dilution heats, were carried out by making identical injections in the absence of protein. All titrations were recorded at 25 °C. The dilution heats were subtracted from the corresponding total heats of reaction to obtain the reaction heats. The titration data were analyzed by the NanoAnalyza software. The data of Zn^{2+} binding to the two single mutants (H244A and H266A) and the wild type C-terminal domain were fit to the independent and multiple site model, respectively.

3. Results

3.1. pH-dependent secondary structure and thermostability of the C-terminal domain

As shown in Supplementary Fig. S1, the far-UV CD spectra of the protein showed two pronounced double minima at 222 and 208 nm with a range of pH 5–8, characteristic of α-helical secondary structure [23]. Although the characteristic double minima of α-helix remained, the α-helical content was decreased with a pH increase (Supplementary Fig. S1 and Table S1). The ratios of $\theta_{222}/\theta_{208}$ that provide the information on the likelihood of the coiled-coil dissociation were more than 1.0 (Supplementary Table S1), indicating that the protein remains a dimeric structure between pH 5 and 8 [24,25], which is consistent with the result from analytical ultracentrifugation [26].

The thermal-melt curves of the C-terminal domain in response to pH values were shown in Fig. 1A and C. At pH 5 and 6, the fractions unfolded were sharply increased from 45 and 37 to 65 and 58 °C, and reached a plateau at 75 and 62 °C (Fig. 1A), respectively. However, at pH 7 and 8, the fraction unfolded was increased from 37 and 25 to 58 and 65 °C, and reached a plateau at 68 and 75 °C (Fig. 1C), respectively. The mid-point temperatures (T_m) of the protein in response to pH values were calculated and listed in Table 1.

Van't Hoff plots calculated from the data of Fig. 1A and C were shown in Fig. 1B and D, respectively. The enthalpy change (ΔH) of transition at any particular temperature will be equal to the slope of these curves times the gas constant (R = 8.314 J/mol K) [27,28]. At T_m, the enthalpy changes (ΔH_m) of unfolding of the protein were 57.9, 56.2, 53.8 and 28.6 kJ mol^{-1} at pH 5, 6, 7 and 8, respectively. The thermodynamic parameters obtained from the thermal stability curves of the protein at different pH values at T_m were summarized in Table 1.

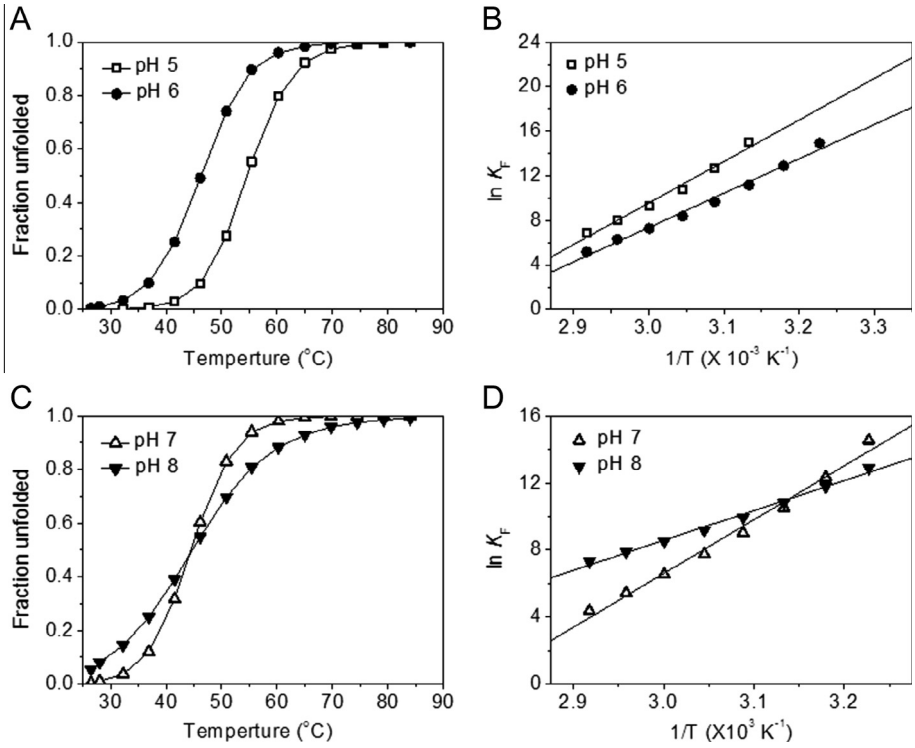

Fig. 1. Effect of pH on coiled-coil thermostability of the C-terminal domain of Hv1. (A and C) Thermal melting profiles of the C-terminal domain at pH 5 (□), 6 (●), 7 (Δ) and 8 (▼). (B and D) Linear fit to the transition zone of data in Fig. 1A and C, respectively. In all experiments, the concentrations of the C-terminal domain is 15 μM.

Table 1
pH-dependent thermodynamic data of the C terminus of Hv1from thermal melt analysis.[a]

pH	T_m[b] (°C)	ΔH_m[c] (kcal mol^{-1})	ΔG_m[d] (kcal mol^{-1})	ΔS_m[e] (kcal mol^{-1} K^{-1})
5	54.4	57.9	−2.24	0.17
6	46.4	56.2	−4.49	0.19
7	44.5	53.8	−6.52	0.19
8	44.6	28.6	−3.16	0.10

[a] Data were obtained at 30 °C, and the concentration of C terminus is about 15 μM.
[b] T_m is the temperature at which the fraction of folded is 50%.
[c] The enthalpy change.
[d] The free energy change.
[e] The entropy change.

Table 2
Summary of thermodynamic parameters for Zn^{2+} binding to the C-terminal domain of Hv1 at 25 °C.

Protein	K_a[a] (×10^4 M^{-1})	n[b]	ΔG[c] (kJ mol^{-1})	ΔH[d] (kJ mol^{-1})	ΔS[e] (J mol^{-1} K^{-1})
C-Hv1 WT	9.58 ± 0.47[f]	0.40 ± 0.11[f]	−31.4[f]	−20.5 ± 4.6[f]	36.5[f]
	1.85 ± 0.39[g]	0.89 ± 0.13[g]	−24.3[g]	25.0 ± 4.1[g]	165.5[g]
H244A/H266A	0.92 ± 0.77	0.92 ± 0.67	−22.5	−2.21 ± 2.14	68.3
H244A (His^{266})	8.27 ± 0.56	0.47 ± 0.08	−27.9	−19.31 ± 4.34	28.9
H266A (His^{244})	10.12 ± 0.92	1.08 ± 0.01	−28.5	44.07 ± 0.73	244.3

[a] K_a is the association constant.
[b] n is the number of ligands bound.
[c] ΔG is the change in free energy.
[d] ΔH is the change in enthalpy.
[e] ΔS is the change in entropy.
[f,g] Thermodynamic parameters for binding site 1 and 2, respectively.

3.2. Zn^{2+} binds to His residues in C-terminus

There are two His residues in the C-terminal domain of Hv1, His^{244} and His^{266}, both of which localize in the accessible region (Fig. 2A). As shown Fig. 2B, Zn^{2+}-induced precipitation of the C-terminal domain of Hv1 (wild type) depended on pH value and the mole ratios of the protein to Zn^{2+}. The precipitation occurred at pH 7.2 and 1:2 mol ratio. The Zn^{2+}-induced precipitation of the protein was not detected when the protein concentration is less than 0.5 mg/ml. The mole ratio of the protein to Zn^{2+} at which

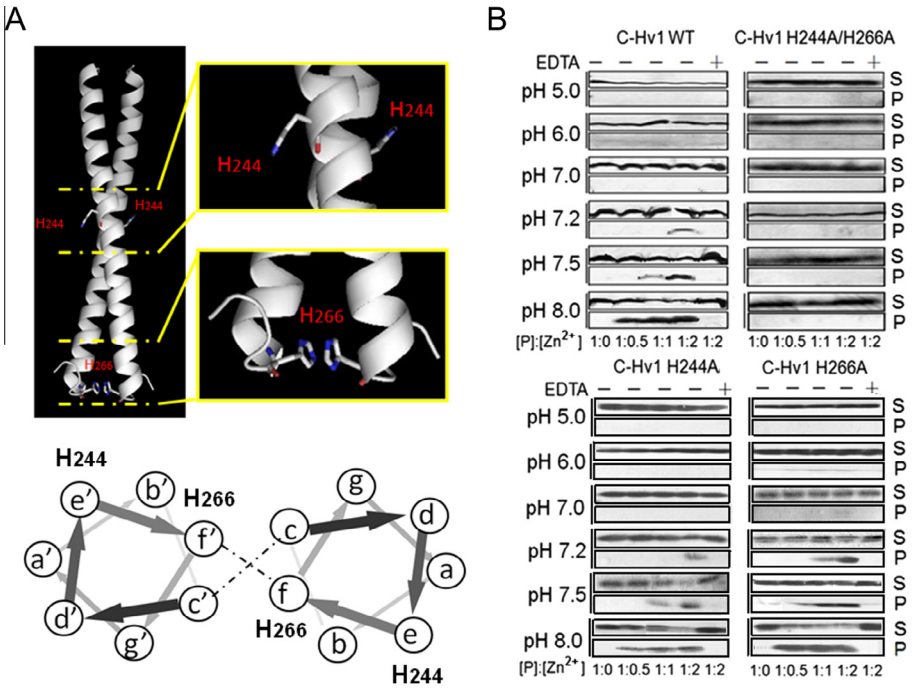

Fig. 2. Zn^{2+} binds to the His residues within the C-terminal domain of Hv1. (A) Locations of His^{244} and His^{266} in the dimeric coiled-coil domain. (B) Zn^{2+}-induced precipitation of the wild type C-terminal domain (C-Hv1 WT), the double mutant H244A/H266A (C-Hv1 H244A/H266A) and two single mutants (H244A and H266A) detected by SDS–PAGE. The concentration of the protein is 0.5 mg/ml (~75 μM). S, supernatant; P, precipitate.

precipitation appeared was increased with a pH increase (Fig. 2B). The precipitation disappeared when EDTA was added into the mixture solution of the protein with Zn^{2+}, indicating that Zn^{2+} interacts with the C-terminal domain of Hv1 and induces the protein precipitation. The mutants H244A and H266A behaved like the wild type protein (Fig. 2B). However, the Zn^{2+}-induced precipitation of the double mutant H244A/H266A did not occur at all from pH 5–8, indicating that Zn^{2+} interacts with both His^{244} and His^{266} residues.

3.3. Thermodynamics signature of Zn^{2+} binding to the His residues

To further confirm the binding sites of Zn^{2+} within the C-terminal domain of Hv1, ITC experiments were carried out at 25 °C. The heat changes revealing the binding events are shown in the upper panels of Fig. 3. Plots of the integrated heat are displayed in the lower panels. As shown in Fig. 3A, Zn^{2+} binding to the WT protein began with an exothermic heat reaction and transformed to an endothermic reaction at the end. The two different reactions that occurred during the Zn^{2+} binding progress suggested that there are at least two Zn^{2+} binding sites being present within the C-terminal domain. The heat change upon Zn^{2+} titration to the H244A/H266A double mutant was shown in Fig. 3B. The exothermic heat reaction was lost and the endothermic reaction sharply decreased, indicating that His^{244} and His^{266} accounted for one of the exothermic and endothermic heat reactions, respectively. Furthermore, the heat change upon Zn^{2+} titration to H244A was a simple exothermic heat reaction (Fig. 3C). In contrast, a simple endothermic heat reaction occurred when H266A was titrated with $ZnCl_2$ solution (Fig. 3D). Taken together, both His^{244} and His^{266} were Zn^{2+} binding sites. The binding of Zn^{2+} to His^{244} (mutant H266A) was an endothermic heat reaction, while the binding of Zn^{2+} to His^{266} (mutant H244A) was an exothermic heat reaction.

The integrated heat data of Zn^{2+} binding to WT protein were fitted to a binding model containing a set of two independent binding sites. The fit to this binding model yielded K_{a1} value of $(9.58 \pm 0.35) \times 10^4\ M^{-1}$ and K_{a2} value of $(1.85 \pm 0.56) \times 10^4\ M^{-1}$ to site 1 (His^{266}) and site 2(His^{244}) with respective n_1 value of 0.40 ± 0.09 and n_2 value of 0.89 (Table 2). Fits of the heat data for Zn^{2+} titration to the mutants (H244A, H266A and the H244A/H266A double mutant) were carried out using the model which entails a single binding event. K_a and binding stoichiometry n values for each titration were summarized in Table 2. The association constant of Zn^{2+} binding to the H244A/H266A double mutant was $(0.92 \pm 0.77) \times 10^4\ M^{-1}$ with a n value of 0.92 ± 0.6, whereas the fits of Zn^{2+} binding to His^{244} (H266A) and His^{266} (H244A) resulted in a higher K_a and n in agreement with those of the WT, specifically $(10.1 \pm 0.92) \times 10^4\ M^{-1}$ and 1.08 ± 0.01 for His^{244} (H266A), $(8.27 \pm 2.37) \times 10^4\ M^{-1}$ and 0.47 ± 0.08 for His^{266} (H244A).

4. Discussion

The voltage-gated proton channel Hv1 mediates charge compensation during the oxidative burst of phagocytosis [29–32] and has been implicated in modulation of several physiological and pathological processes [33–38]. Zn^{2+}, as the most characterized inhibitor of Hv1, has been extensively used in the molecular and functional studies of this class of channels. In the present work, we studied the pH-dependent structural stability of the intracellular C-terminal domain of human Hv1 and investigated the binding of Zn^{2+} to the coiled-coil domain by isothermal titration calorimetry (ITC). We found that two His residues His^{244} and His^{266} are indispensable for Zn^{2+} binding.

Hv1 is built out of two subunits arranged as a dimer [8–10]. The intracellular C-terminal domain of Hv1 was found to be responsible for both the channel dimerization and cooperative gating [5,13,14]. The C-terminus was also found to regulate the channel activation kinetics in a temperature-dependent manner [14]. Moreover, the activation and deactivation kinetics of the C-terminus deleted Hv1 are much faster than the full-length dimeric channel [9,14,16,39]. The tail current time constant (τ_{tail}, at −40 mV) is 60 ms for Hv1 without the C-terminal domain and

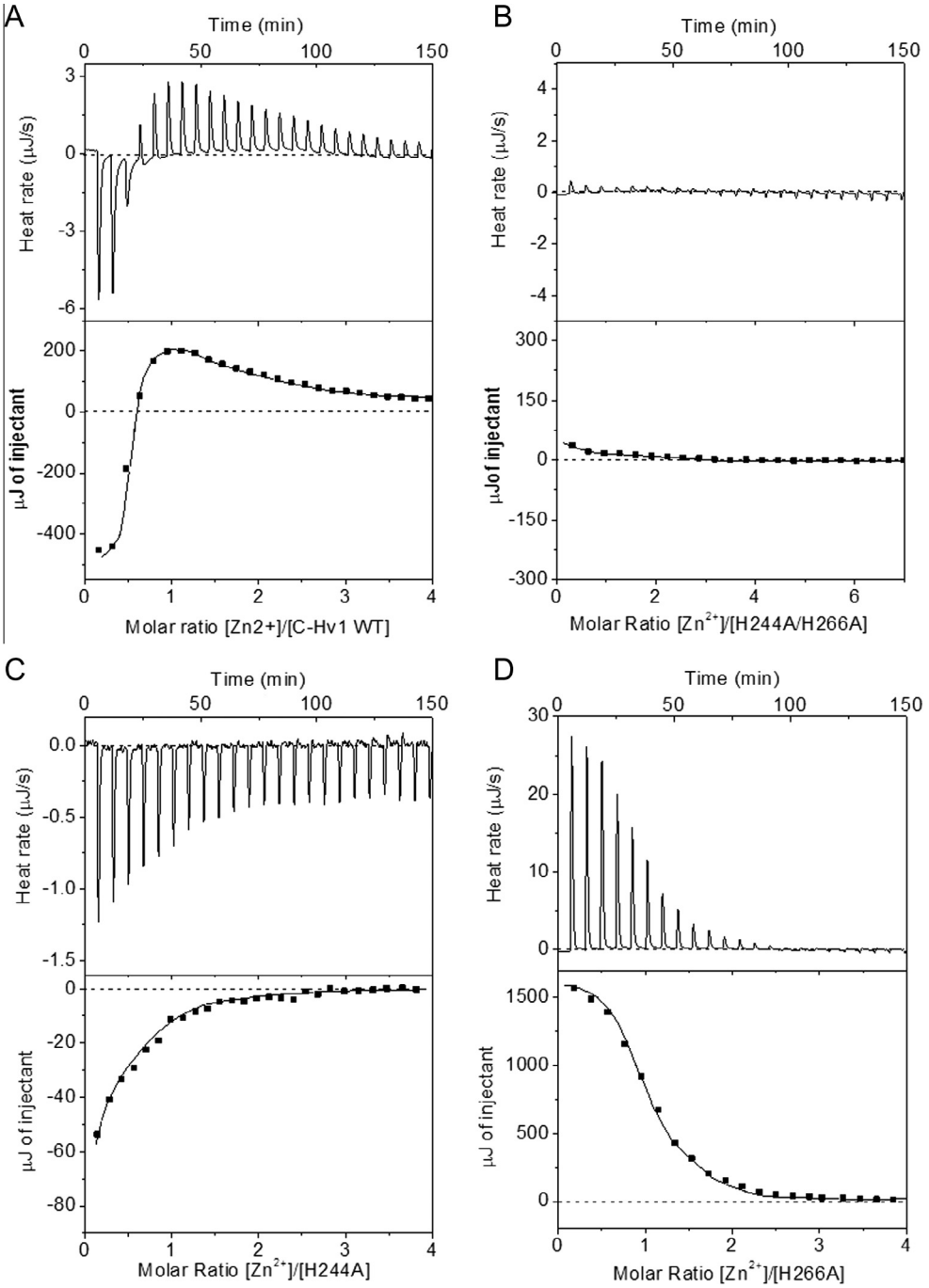

Fig. 3. ITC analyses of Zn^{2+} binding to the C-terminal domain of Hv1. The upper panels show the calorimetric titrations with 8 μl-injections of 2.5 mM $ZnCl_2$ into 0.1 mM the wild type C-terminal domain (A) and 5 mM $ZnCl_2$ into 0.1 mM the double mutant H244A/H266A (B), 0.6 mM $ZnCl_2$ into 0.06 mM H244A mutant (C), and 2.5 mM $ZnCl_2$ into 0.1 mM H266A mutant (D). The lower panels display the integrated heat values from the upper panels as a function of the molar ratio of Zn^{2+} to the corresponding proteins. The exothermic reaction is shown by a negative heat effect, while the endothermic reaction is shown by a positive heat effect. C-Hv1, the wild type C-terminal domain; H244A/H266A, the double H244A/H266A mutant; H244A, the H244A mutant; H266A, the H266A mutant.

370 ms for the full-length Hv1 [4], indicating that the C-terminal domain is involved in the channel closing. At the same time, the channel closing is slowed by internally applied Zn^{2+} and the distinct metal binding sites must exist at the inner surfaces of the channel [16]. In the present work, we found that the secondary structure and thermostability of the C-terminal domain of Hv1 were both pH-sensitive. Furthermore, the α-helical content and thermostability of the C-terminal domain decreased with a pH increase (from pH 5 to 6). At pH 5, the secondary structure and thermostability of the protein also decreased with the binding of Zn^{2+} [17]. At pH 7, the thermo-induced unfolded fraction of the C-terminal domain increased from 37 °C and reached a plateau at 75 °C, while at pH 8, the unfolded fraction of the C-terminal domain in the absent of Zn^{2+} began to increase from 25 °C and then reached a plateau at 80 °C, which is similar with the previous data in the present of Zn^{2+} at pH 7 [17], indicating that the effects of pH increase on the thermostability of the protein are almost same with that of Zn^{2+}-binding.

Titration calorimetry is a universal method for measuring binding affinities. It is capable of characterizing the molecular nature of

macromolecular interactions. In the present work, the interaction between Zn^{2+} and the C-terminal domain of Hv1 was characterized in detail by ITC measurements. For analysis of the data of Zn^{2+} binding to the wild type C-terminal domain, the multiple sites model was used. The multiple sites model is a two-site model in which the ligand binds two chemically distinct sites on a receptor molecule. The independent model, a one-site model that models an interaction of "*n*" ligands with a macromolecule, was used to analyze the data of Zn^{2+} binding to the two single mutants (H244A and H266A). The binding stoichiometry *n* value resulted from the fit of Zn^{2+} binding to the H244A single mutant (His^{266} residue) is 0.47 ± 0.08. His^{266} residue is positioned in the hydrophobic core of the two helix bundles. And the His^{266} residues of the two monomers are ~7.9 Å apart. Thus, Zn^{2+} binding to His^{266} may occur at the dimer interface between the pair of His residues from both subunits, which is similar to external Zn^{2+} binding to His^{140} and His^{193} [16]. In the case of Zn^{2+} binding to H266A mutant (His^{244} residue), His^{244} is localized in the position that makes up the backbone of the coiled-coil structure [14,23]. The fit of Zn^{2+} binding to the H266A single mutant (His^{244} residue) resulted in an *n* value of 1.08 ± 0.01, indicating that Zn^{2+} binding to His^{244} may occur at each subunit in the dimer.

Acknowledgments

This work was supported by National Natural Science Foundation of China (Nos. 30970579 and 31271464), the Ph.D. Programs Foundation of Ministry of Education of China (Nos. 20110031110004 and 20120031110028), and the Basic Science and Advance Technology Research Program of Tianjin (No. 14JCYBJC23400). This research is based on the Cooperative Research Project of Research Institute of Electronics, Shizuoka University.

Appendix A. Supplementary data

Supplementary data associated with this article can be found, in the online version, at http://dx.doi.org/10.1016/j.bbrc.2014.11.060.

References

[1] T.E. DeCoursey, Voltage-gated proton channels and other proton transfer pathways, Physiol. Rev. 83 (2003) 475–579.
[2] I.S. Ramsey, M.M. Moran, J.A. Chong, D.E. Clapham, A voltage-gated proton-selective channel lacking the pore domain, Nature 440 (2006) 1213–1216.
[3] M. Sasaki, M. Takagi, Y. Okamura, A voltage sensor-domain protein is a voltage-gated proton channel, Science 312 (2006) 589–592.
[4] B. Musset, T.E. DeCoursey, Biophysical properties of the voltage-gated proton channel Hv1, WIREs Membr. Transport Signalling 1 (2012) 605–620.
[5] T.E. DeCoursey, Voltage-gated proton channels: molecular biology, physiology, and pathophysiology of the Hv family, Physiol. Rev. 93 (2013) 599–652.
[6] D. Morgan, V.V. Cherny, R. Murphy, B.Z. Katz, T.E. DeCoursey, The pH dependence of NADPH oxidase in human eosinophils, J. Gen. Physiol. 569 (2005) 419–431.
[7] C. Eder, T.E. DeCoursey, Voltage-gated proton channels in microglia, Prog. Neurobiol. 64 (2001) 277–305.
[8] S.Y. Lee, J.A. Letts, R. MacKinnon, Dimeric subunit stoichiometry of the human voltage-dependent proton channel Hv1, Proc. Natl. Acad. Sci. U.S.A. 105 (2008) 7692–7695.
[9] H.P. Koch, T. Kurokawa, Y. Okochi, M. Sasaki, Y. Okamura, H.P. Larsson, Multimeric nature of voltage-gated proton channels, Proc. Natl. Acad. Sci. U.S.A. 105 (2008) 9111–9116.
[10] F. Tombola, M.H. Ulbrich, E.Y. Isacoff, The voltage-gated proton channel Hv1 has two pores, each controlled by one voltage sensor, Neuron 58 (2008) 546–556.
[11] C. Gonzalez, H.P. Koch, B.M. Drum, H.P. Larsson, Strong cooperativity between subunits in voltage-gated proton channels, Nat. Struct. Mol. Biol. 17 (2009) 51–56.
[12] F. Tombola, M.H. Ulbrich, S.C. Kohout, E.Y. Isacoff, The opening of the two pores of the Hv1 voltage-gated proton channel is tuned by cooperativity, Nat. Struct. Mol. Biol. 17 (2010) 44–50.
[13] Y. Fujiwara, T. Kurokawa, K. Takeshita, M. Kobayashi, A. Nakagawa, Y. Okamura, Stability of the cytoplasmic dimer assembly regulates the thermosensitive gating of the voltage-gated H^+ channel, Biophys. J. 100 (2011) 348a.
[14] Y. Fujiwara, T. Kurokawa, K. Takeshita, M. Kobayashi, Y. Okochi, A. Nakagawa, Y. Okamura, The cytoplasmic coiled-coil mediates cooperative gating temperature sensitivity in the voltage-gated H^+ channel Hv1, Nat. Commun. 3 (2012) 816.
[15] V.V. Cherny, T.E. DeCoursey, PH-dependent inhibition of voltage-gated H^+ currents in rat alveolar epithelial cells by Zn^{2+} and other divalent cations, J. Gen. Physiol. 114 (1999) 819–838.
[16] B. Musset, S.M.E. Smith, S. Rajan, V.V. Cherny, S. Sujai, D. Morgan, T.E. DeCoursey, Zinc inhibition of monomeric and dimeric proton channels suggests cooperative gating, J. Physiol. 588 (2010) 1435–1449.
[17] Q. Zhao, Y. Zhang, S.J. Li, Interaction of divalent metal ions with the carboxyl-terminal domain of human voltage-gated proton channel Hv1, Biometals 27 (2014) 793–802.
[18] F.S. Steven, M.M. Griffin, B.S. Brown, T.P. Hulley, Aggregation of fibrinogen molecules by metal ions, Int. J. Biol. Macromol. 4 (1982) 367–369.
[19] H.V. Iyer, T.M. Przybycien, Metal affinity protein precipitation-effects of mixing, protein concentration, and modifiers on protein fractionation, Biotechnol. Bioeng. 48 (1995) 324–332.
[20] T.H. Yang, J.L. Cleland, X. Lam, J.D. Meyer, L.S. Jones, T. Randolph, M.C. Manning, J.F. Carpenter, Effect of zinc binding and precipitation on structures of recombinant human growth hormone and nerve growth factor, J. Pharm. Sci. 89 (2000) 1480–1485.
[21] S.J. Li, Q. Zhao, Q. Zhou, Y. Zhai, Expression, purification, crystallization and preliminary crystallographic study of the carboxyl-terminal domain of the human voltage-gated proton channel Hv1, Acta Crystallogr. F65 (2009) 279–281.
[22] J.M. Mason, U.B. Hagemann, K.M. Arndt, Improved stability of the jun-fos activator protein-1 coiled-coil motif a stopped-flow circular dichroism kinetic analysis, J. Biol. Chem. 282 (2007) 23015–23024.
[23] V.P. Saxena, D.B. Wetlaufer, A new basis for interpreting the circular dichroism spectra of proteins, Proc. Natl. Acad. Sci. U.S.A. 68 (1971) 969–972.
[24] S.C. Kwok, R.S. Hodges, Stabilizing and destabilizing clusters in the hydrophobic core of long two-stranded alpha-helical coiled-coils, J. Biol. Chem. 279 (2004) 21576–21588.
[25] E.N. Shepherd, H.N. Hoang, G. Abbenante, D.P. Fairli, Single turn peptide alpha helices with exceptional stability in water, J. Am. Chem. Soc. 127 (2005) 2974–2983.
[26] S.J. Li, Q. Zhao, Q. Zhou, H. Unno, Y. Zhai, F. Sun, The role and structure of the carboxyl-terminal domain of the human voltage-gated proton channel Hv1, J. Biol. Chem. 285 (2010) 12047–12054.
[27] N.J. Greenfield, Using circular dichroism collected as a function of temperature to determine the thermodynamics of protein unfolding and binding interactions, Nat. Protoc. 1 (2006) 2527–2535.
[28] J.F. Brandts, The thermodynamics of protein denaturation. I. The denaturation of chymotrypsinogen, J. Am. Chem. Soc. 86 (1964) 4291–4302.
[29] I.S. Ramsey, E. Ruchti, J.S. Kaczmarek, D.E. Clapham, Hv1 proton channels are required for high-level NADPH oxidase-dependent superoxide production during the phagocyte respiratory burst, Proc. Natl. Acad. Sci. U.S.A. 106 (2009) 7642–7647.
[30] D. Morgan, M. Capasso, B. Musset, V.V. Cherny, E. Ríos, M.J.S. Dyer, T.E. DeCoursey, Voltage-gated proton channels maintain pH in human neutrophils during phagocytosis, Proc. Natl. Acad. Sci. U.S.A. 106 (2009) 18022–18027.
[31] Y. Okochi, M. Sasaki, H. Iwasaki, Y. Okamura, Voltage-gated proton channel is expressed on phagosomes, Biochem. Biophys. Res. Commun. 382 (2009) 274–279.
[32] M. Capasso, M.K. Bhamrah, T. Henley, R.S. Boyd, C. Langlais, K. Cain, D. Dinsdale, K. Pulford, M. Khan, B. Musset, et al., HVCN1 modulates BCR signal strength via regulation of BCR-dependent generation of reactive oxygen species, Nat. Immunol. 11 (2010) 265–272.
[33] L.J. Wu, G. Wu, M.R.A. Sharif, A. Baker, Y. Jia, F.H. Fahey, H.R. Luo, E.P. Feener, D.E. Clapham, The voltage-gated proton channel Hv1 enhances brain damage from ischemic stroke, Nat. Neurosci. 15 (2012) 565–573.
[34] P.V. Lishko, I.L. Botchkina, A. Fedorenko, Y. Kirichok, Acid extrusion from human spermatozoa is mediated by flagellar voltage-gated proton channel, Cell 140 (2010) 327–337.
[35] Y. Wang, S.J. Li, J. Pan, Y. Che, J. Yin, Q. Zhao, Specific expression of the human voltage-gated proton channel Hv1 in highly metastatic breast cancer cells, promotes tumor progression and metastasis, Biochem. Biophys. Res. Commun. 412 (2011) 353–359.
[36] Y. Wang, S.J. Li, X. Wu, Y. Che, Q. Li, Clinicopathological and biological significance of human voltage-gated proton channel Hv1 protein overexpression in breast cancer, J. Biol. Chem. 287 (2012) 13877–13888.
[37] Y. Wang, X. Wu, Q. Li, S. Zhang, S.J. Li, Human voltage-gated proton channel Hv1: a new potential biomarker for diagnosis and prognosis of colorectal cancer, PLoS ONE 8 (2013) e70550.
[38] Y. Wang, S. Zhang, S.J. Li, Zn^{2+} induces apoptosis in human highly metastatic SHG-44 glioma cells, through inhibiting activity of the voltage-gated proton channel Hv1, Biochem. Biophys. Res. Commun. 438 (2013) 312–317.
[39] B. Musset, S.M.E. Smith, S. Rajan, V.V. Cherny, D. Morgan, T.E. DeCoursey, Oligomerization of the voltage-gated proton channel, Channels 4 (2010) 260–265.